Tryptophan 86 of the α Subunit in the *Torpedo* Nicotinic Acetylcholine Receptor Is Important for Channel Activation by the Bisquaternary Ligand Suberyldicholine†

Ankur Kapur, Martin Davies, William F. Dryden, and Susan M. J. Dunn*

Department of Pharmacology, Faculty of Medicine and Dentistry, University of Alberta, Edmonton, Alberta, Canada T6G 2H7

Received February 23, 2006; Revised Manuscript Received June 2, 2006

ABSTRACT: Suberyldicholine, a bisquaternary compound, is a potent nicotinic acetylcholine receptor agonist. Previously, we suggested that at least some of the unusual binding properties of this ligand may be a consequence of its ability to cross-link two binding "subsites" within each of the high-affinity agonist binding domains [Dunn, S. M. J., and Raftery, M. A. (1997) *Biochemistry 36*, 3846−3853]. Tryptophan 86 of the α subunit has previously been implicated in the binding of agonist to this receptor. However, on the basis of the crystal structure of a homologous acetylcholine binding protein, this residue is predicted to lie 15−20 Å from the high-affinity site, i.e., a distance that approximates the interonium distance of suberyldicholine. Tryptophan 86 was mutated to either an alanine or a phenylalanine, and the mutated subunit was coexpressed with wild-type *β*, *γ*, and *δ* subunits in *Xenopus* oocytes. Although the alanine mutation resulted in a loss of receptor expression, the αW86F mutant receptor was expressed on the oocyte surface, albeit with a much reduced efficiency. Acetylcholine-evoked currents of the αW86F receptor were not significantly different from those of the wild type with respect to the concentration dependence of channel activation, receptor desensitization, or D-tubocurarine inhibition. In contrast, the EC_{50} for suberyldicholine-mediated activation of the αW86F receptor was increased by ∼500-fold. Furthermore, suberyldicholine-evoked currents in the mutant receptor did not desensitize and were insensitive to block by D-tubocurarine. Thus, tryptophan 86 of the *Torpedo* receptor α subunit may be part of a subsite for recognition of suberyldicholine and other bisquaternary ligands.

The peripheral nicotinic acetylcholine receptor (nAChR)[1] is the prototypical member of the Cys-loop ligand-gated ion channel (LGIC) family that includes the $GABA_A$, $5HT_3$, and glycine receptors (*1*). The *Torpedo* nAChR is a transmembrane pentameric protein complex ($\alpha_2\beta\gamma\delta$) in which the subunits are arranged pseudosymmetrically around a central cation-selective ion channel (*2*, *3*). Biochemical and mutational studies have revealed that high-affinity binding sites for agonists and competitive antagonists are formed by at least six discontiguous "loops" of amino acids (loops A−F) that lie at the α−*γ* and α−*δ* subunit interfaces (*1*, *4*, *5*). Within the α subunits, several key amino acids have been implicated in ligand binding. These include Y93 (loop A), W149 (loop B), and Y190, C192, C193, and Y198 (loop C) (*6*−*9*). Loops D−F are contributed by the neighboring *γ* or *δ* subunit, and at least for some antagonists, the distinct recognition properties of these subunits confer nonequivalence to the binding sites (*10*, *11*).

Although the location of high-affinity binding sites at subunit−subunit interfaces had been predicted from a wealth of experimental data, only recently was this given a physical reality with the crystallization of a related protein, the acetylcholine binding protein (AChBP) (*12*). This protein, which is secreted by glial cells of the snail *Lymnaea stagnalis* (*13*), is a soluble homopentamer that is homologous to the extracellular amino-terminal domains of the nAChR and other members of the LGIC family. Its structure confirms that the stretches of amino acids that have been implicated in ligand binding within the LGIC family lie at subunit−subunit interfaces. Thus, the AChBP is a valuable template on which to model these binding sites.

Suberyldicholine (SbCh) is a potent agonist of the nAChR (*14*, *15*). We previously investigated differences in binding of [^{3}H]ACh and [^{3}H]SbCh to the membrane-bound *Torpedo* receptor (*16*, *17*). Under equilibrium conditions, each ligand binds to two receptor sites with similarly high affinity (K_d ∼ 15 nM). However, the kinetics of binding of the two ligands are significantly different. In dissociation experiments, micromolar concentrations of unlabeled ligands accelerated the rate of dissociation of [^{3}H]ACh from the high-affinity sites to which it had previously been bound (*16*), Detailed studies of this phenomenon led to a model in which each of the two high-affinity sites is made up of two physically distinct "subsites" which, for the sake of simplicity, were termed sites A and B. With [^{3}H]ACh initially occupying site A, the subsequent binding of unlabeled ligand to site B induces a conformational transition that displaces [^{3}H]ACh from site A. Thus, for ACh, the two subsites are allosterically coupled but mutually exclusive at equilibrium. In contrast, the dissociation of [^{3}H]SbCh was relatively

† This work was supported by the Canadian Institutes of Health Research.

* To whom correspondence should be addressed. Telephone: (780) 492-3414. Fax: (780) 492-4325. E-mail: susan.dunn@ualberta.ca.

[1] Abbreviations: ACh, acetylcholine; AChBP, acetylcholine binding protein; α-BgTx, α-bungarotoxin; GABA, *γ*-aminobutyric acid; LGIC, ligand-gated ion channel; nAChR, nicotinic acetylcholine receptor; SbCh, suberyldicholine; dTC, D-tubocurarine; SEM, standard error of the mean; WT, wild-type.

10.1021/bi0603773 CCC: $33.50 © 2006 American Chemical Society
Published on Web 08/03/2006

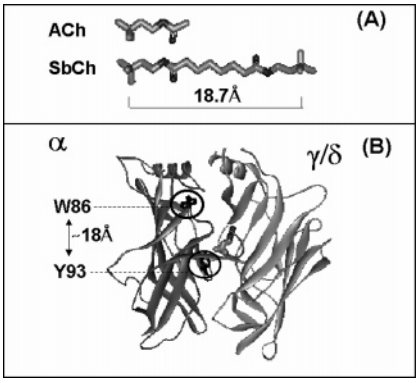

FIGURE 1: Suberyldicholine and possible involvement of residue αW86 in binding. (A) Structures of ACh and SbCh showing their relative size in their extended conformations and the estimated interonium distance of SbCh. (B) Side view of the *Torpedo* nAChR α−γ (or δ) interface based on the crystal structure of AChBP. The figure shows the predicted locations of Y93 and W86 in the α subunit and also the predicted orientation of carbamylcholine within the binding site (shown as a stick orientation) based on the crystal structure of the AChBP−carbamylcholine complex (see ref *18*).

resistant to any accelerating effects of unlabeled ligands. It was, therefore, suggested that this large bisquaternary ligand (see Figure 1A) may be able to bridge the two subsites (*16*). Further examination of the association kinetics for ACh and a series of bisquaternary suberyldicholine analogues placed physical constraints on the distance between these putative subsites. It was determined that pimelyldicholine, which is one methylene group shorter than SbCh, is of sufficient length to display SbCh-like binding behavior (*17*).

Clues about the location of the putative secondary site for SbCh have come from the results of photoaffinity labeling of *Torpedo* nAChR by the competitive antagonist *p*-[^{3}H]-dimethylaminobenzene diazonium fluoroborate. Tyrosine 93 lying in loop A of the α subunit (αY93) was the major site of labeling (*8*). However, αW86 was also labeled, albeit to a low extent, and this led to its inconclusive identification as a binding site residue. Examination of the crystal structure of the AChBP (*12*; see Figure 1B) shows that the residue in the homologous position (W82) lies approximately 18 Å from Y93 and the other residues that have been identified as being important in high-affinity agonist and antagonist binding (*18*).

In the study presented here, we investigated W86 of the *Torpedo* nAChR α subunit for its possible contributions to formation of a binding subsite for SbCh and related bisquaternary agonists. The results reveal that this residue is very important for activation of the receptor by SbCh but has minimal influence on ACh-induced responses.

EXPERIMENTAL PROCEDURES

Materials. ACh, SbCh, α-bungarotoxin (α-BgTx), and D-tubocurarine (dTC) were obtained from Sigma-RBA (Natick, MA). [^{125}I]-α-BgTx (2000 Ci/mmol) was from Amersham Life Science (Arlington Heights, IL). Restriction enzymes and cRNA transcript preparation materials were purchased from Invitrogen (Burlington, ON), Promega (Madison, WI), or New England Biolabs (Pickering, ON). *Pfu* Turbo DNA polymerase for mutagenesis experiments was from Stratagene (La Jolla, CA). All other chemicals were obtained from Sigma or other standard sources. The α, β (in the SP64 plasmid), and δ subunit (in the SP65 plasmid) cDNA clones of the *Torpedo* nAChR were kindly provided by H. A. Lester (California Institute of Technology, Pasadena, CA), and the γ subunit cDNA (in the SP64-based plasmid, pMXT) was a generous gift from J. B. Cohen (Harvard Medical School, Boston, MA).

In Vitro Transcription and Site-Directed Mutagenesis. The plasmid cDNAs were linearized by digestion with *Eco*RI (wild-type and mutant α subunits), *Fsp*I (β subunit), or *Xba*I (γ and δ subunits). In vitro cRNA transcription was performed using the methods described by Goldin and Sumikawa (*19*). Briefly, the linearized cDNA (5 μg) templates were transcribed in vitro by SP6 RNA polymerase (Promega) in the presence of ribonucleotide triphosphates (NTP mix, Invitrogen) and RNA capping analogue (New England Biolabs). The RNA transcripts were extracted using a 25:24:1 (v/v) phenol/chloroform/isoamyl alcohol mixture. The final RNA pellets were resuspended in diethyl pyrocarbonate-treated water at a concentration of 1 μg/μL and were stored at −86 °C prior to use. The α subunit mutants (W86F and W86A) were constructed using Stratagene's QuikChange site-directed mutagenesis protocol. Synthetic oligonucleotide mutagenic primers were typically 27−35 bp long (with 10−15 bp on either side of the mismatch region). Restriction endonuclease digestion and DNA sequencing subsequently verified the presence of the mutation.

Expression in Xenopus Oocytes and Electrophysiology. Isolated, follicle-free oocytes were microinjected with 50 ng of total subunit cRNAs in an α:β:γ:δ ratio of 2:1:1:1. Oocytes were maintained in ND96 buffer [96 mM NaCl, 2 mM KCl, 1.8 mM $CaCl_2$, 1 mM $MgCl_2$, and 5 mM HEPES (pH 7.6)] supplemented with 50 μg/mL gentamicin at 14 °C for at least 48 h prior to recording. Currents elicited by bath application of ACh or SbCh were measured by standard two-electrode voltage clamp techniques using a GeneClamp 500 amplifier (Axon Instruments, Foster City, CA) and a holding potential of −60 mV. Electrodes were filled with 3 M KCl, and those with resistances of 0.5−3.0 MΩ were used. The recording chamber was perfused continuously (at a flow rate of ∼5 mL/min) with low-calcium ND96 buffer (as described above but with the concentration of $CaCl_2$ reduced to 0.1 mM) supplemented with 1 μM atropine (pH 7.6). Atropine was included in the perfusion buffer to block endogenous muscarinic receptors present in the oocytes (*20*), and a low level of Ca^{2+} was used to reduce the extent of receptor desensitization (*21*). Agonist-evoked responses were measured by applying drug via the perfusion system for 15−20 s or longer as indicated in the text. A 15 min washout period between applications was used to ensure recovery from desensitization. To measure the concentration dependence of D-tubocurarine (dTC) effects, oocytes were preperfused with varying concentrations of dTC for 2 min before the response was initiated by application of a solution containing ACh or SbCh, at concentrations eliciting 50% (EC_{50}) or 90% (EC_{90}) of the maximum response, and including the same concentration of dTC that was used for preincubation.

Radioligand Binding of [^{125}I]-α-BgTx to Intact Oocytes. Binding assays were performed on individual oocytes that had previously been used for electrophysiological recording. To measure the density of α-BgTx sites expressed on the surface, oocytes were incubated with 5 nM [^{125}I]-α-BgTx

in a final volume of 100 μL of low-Ca^{2+} ND96 buffer (supplemented with 5 mg/mL bovine serum albumin) for 2 h (*22*, *23*). Excess unbound toxin was removed by washing the oocytes three times with 1 mL of ice-cold low-Ca^{2+} ND96 buffer. Nonspecific binding was assessed by incubating uninjected oocytes with [^{125}I]-α-BgTx. Nonspecific binding assessed in the presence of excess cold ACh was comparable to that estimated using uninjected oocytes (data not shown). Using these data, the maximum currents (I_{max}) measured for wild-type and mutant receptors were normalized to the concentration of binding sites in terms of nanoamperes per femtomole.

Data and Statistical Analysis. Competition and concentration−effect curves for both electrophysiological and radioligand binding experiments were analyzed by nonlinear regression techniques using Prism version 3.0 (GraphPad, San Diego, CA). Data from individual oocytes were normalized to the I_{max} value obtained for that oocyte.

For receptor activation, concentration−effect curves for agonist activation were analyzed using the following equation:

$$I = I_{max}[L]^n/(EC_{50} + [L])^n$$

where I is the measured agonist-evoked current, [L] is the agonist concentration, EC_{50} is the agonist concentration that evokes half the maximal current (I_{max}), and n is the Hill coefficient. In each experiment, the current (I) was normalized to the I_{max} and the normalized data are presented as the percent response to plot concentration−effect curves.

The IC_{50} was determined from competition−inhibition curves by fitting to the following equation:

$$f = 100/[1 + ([X]/IC_{50})^n]$$

where f is the fractional (%) response remaining in the presence of inhibitor at concentration [X], IC_{50} is the inhibitor concentration that reduced the amplitude of the ACh-evoked current by 50%, and n is the Hill coefficient. ACh inhibition of the initial rate of [^{125}I]-α-BgTx binding was also fit by the equation given above.

The K_I(apparent) value was calculated using the Cheng−Prusoff equation (*24*):

$$K_I = IC_{50}/(1 + [L]/EC_{50})$$

where [L] is the agonist concentration used in the experiment and EC_{50} is the agonist concentration that evokes half the maximal current.

Statistical analysis was performed using one-way analysis of variance (ANOVA) followed by Dunnett's post test to determine the level of significance.

RESULTS

Functional Effects of αW86 Mutations on Agonist Responses. The functional responses of wild-type and mutant receptors expressed in *Xenopus* oocytes were studied using two-electrode voltage clamp techniques. Figure 2 shows concentration−effect curves for ACh and SbCh activation of receptor subtypes. In the wild-type nAChR, both ACh and SbCh evoked a concentration-dependent current characterized by EC_{50} values of ~24 μM (n_H = 1.6) and ~3 μM (n_H = 1.4), respectively (see Table 1). Thus, in this expression system, SbCh is approximately 8-fold more potent than ACh. However, as described below, the maximum amplitude of the SbCh-evoked currents was significantly lower than that for ACh, suggesting that it acts as a partial agonist of the *Torpedo* nAChR. Receptors carrying the αW86A mutation failed to respond to ACh, even at concentrations as high as 10 mM. In contrast, the αW86F mutant receptors were functional, although the maximum observed currents were much lower than those mediated by the wild-type receptor. This is likely to be a consequence of reduced levels of receptor expression (see below). Although the αW86F mutation resulted in an only small and insignificant (~2-fold) shift in the EC_{50} for ACh-evoked channel

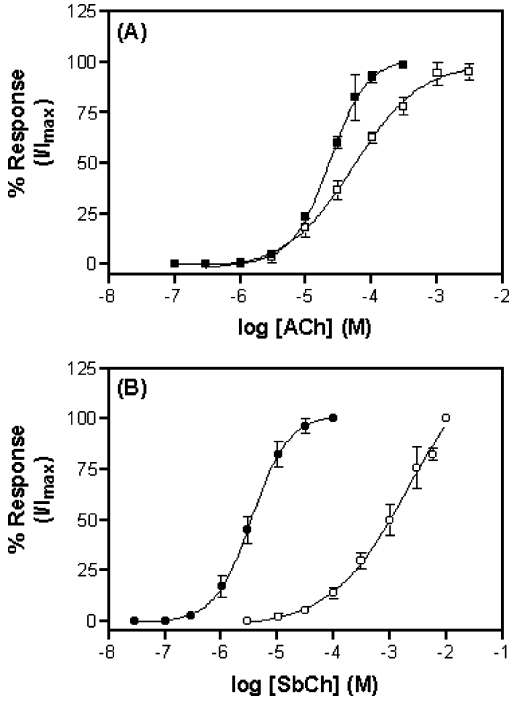

FIGURE 2: Activation of wild-type and αW86F mutant receptors. (A) ACh concentration−effect curves obtained from oocytes expressing the WT (■) and αW86F (□) nAChR. (B) SbCh concentration−effect curves obtained from oocytes expressing WT (●) and αW86F (○). Data are normalized to I_{max} for each individual point. The data represent the means ± SEM from at least three oocytes. The data obtained from curve fitting are summarized in Table 1.

Table 1: Concentration−Effect Data for Acetylcholine and Suberyldicholine Activation of Wild-Type and Mutant Receptors Expressed in *Xenopus* Oocytes[a]

	log EC_{50} ± SEM (M)	EC_{50} (μM)	n_H ± SEM	EC_{50}Mut/ EC_{50}WT
ACh				
WT	−4.61 ± 0.04 (9)	24.3	1.6 ± 0.1	1
αW86F	−4.28 ± 0.08 (4)	52.5	0.9 ± 0.1[b]	2.2
suberyldicholine				
WT	−5.47 ± 0.08 (3)	3.38	1.4 ± 0.04	1
αW86F	−2.77 ± 0.16 (5)[b]	680	0.7 ± 0.04[b]	−500

[a] Data represent the mean ± SEM. Values for the log EC_{50} and Hill coefficient (n_H) were determined from concentration−effect curves using Prism. The log EC_{50} and Hill coefficient values from individual oocytes were averaged to generate final mean estimates. The value in parentheses is the number of oocytes used for each receptor type. Statistical analysis was performed by comparing the log EC_{50} and n_H values of the mutant receptors to those of the wild-type nAChR using one-way ANOVA followed by Dunnett's post test. [b] $p < 0.001$.

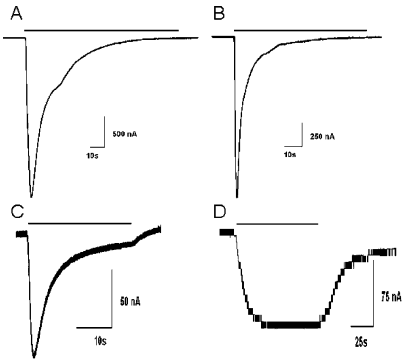

FIGURE 3: Representative current traces showing ACh and SbCh activation of *Xenopus* oocytes expressing wild-type WT and αW86F mutant nAChRs. The concentrations of agonists that were used were those that elicited a maximal response at each subtype except for the effects of SbCh on the mutant receptor where the maximum practical concentration (10 mM) was used. The traces show the activation of the WT receptor by (A) ACh and (B) SbCh and activation of the W86F mutant receptor by (C) ACh and (D) SbCh. The bar above the current trace represents agonist application.

activation (to ~53 μM), this mutation caused a dramatic (>500-fold) decrease in SbCh sensitivity (see Figure 2 and Table 1). It should be noted that the estimates of the parameters for SbCh activation of the mutant receptor (Table 1) are subject to large errors due to the low amplitude of the current responses and limitations on the highest concentrations of SbCh that could be used. The very high concentrations of SbCh required to activate the mutant receptor raise the question of whether the observed responses are receptor-mediated or are an artifact of the *Xenopus* oocyte expression system. However, such high concentrations of SbCh failed to evoke conductance changes in uninjected oocytes, suggesting that the responses are indeed a property of the mutant nAChRs. The Hill coefficients for both ACh- and SbCh-induced activation of the αW86F mutant receptor were significantly reduced (to 0.9 and 0.7, respectively) compared to the wild-type nAChR value (Table 1), suggesting a reduced cooperativity of the responses.

Currents mediated by the wild-type receptor showed rapid desensitization during exposure to ACh or SbCh (Figure 3). However, in the receptor carrying the αW86F mutation, although the ACh-elicited current desensitized, the SbCh-evoked currents failed to exhibit appreciable desensitization after reaching their peak amplitude (see Figure 3D). Also shown in this figure is the very slow activation of this mutant receptor by SbCh. Peak currents in response to SbCh were reached only after an at least 30 s exposure to SbCh in contrast to the very rapid activation of the wild-type nAChR (Figure 3B).

Effects of the αW86F Mutation on D-Tubocurarine Inhibition. We further examined the ability of the competitive antagonist, dTC, to inhibit agonist-evoked currents in wild-type and mutant receptors (Figure 4). Pre-perfusion of both the wild-type and αW86F mutant nAChR with dTC resulted in a complete concentration-dependent inhibition of ACh-evoked currents (K_I ~ 43 nM; see Table 2). In the case of the wild-type receptor, dTC inhibition of SbCh-induced currents (K_I ~ 58 nM) had similar characteristics. In marked contrast, SbCh-evoked currents in the mutant receptor were insensitive to dTC inhibition (Figure 4 and Table 2).

Effects of the αW86F Mutation on Receptor Expression. A major problem in studying the receptor carrying the

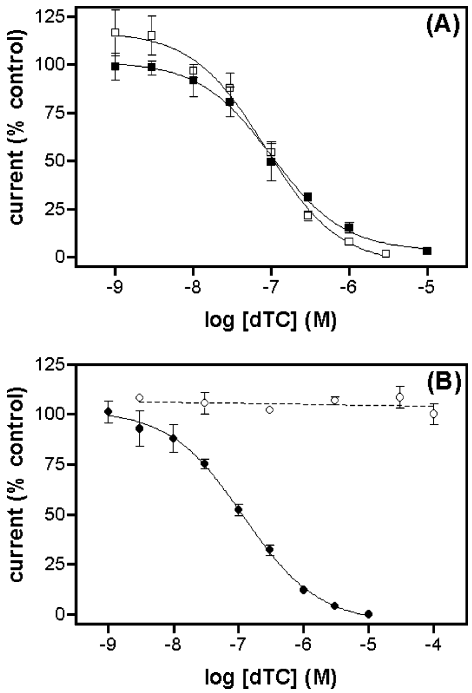

FIGURE 4: Concentration-dependent inhibition of agonist-evoked currents by dTC in oocytes expressing the wild-type and αW86F mutant receptors. (A) Effect of dTC on the ACh-evoked current in WT (■) and αW86F (□). (B) Effect of dTC on the SbCh-evoked current in WT (●) and αW86F (○). The ACh and suberyldicholine concentrations used in these experiments corresponded to their EC_{50} values for activation (Table 1) except in the case of ACh activation of αW86F, where an EC_{90} was used to elicit higher-amplitude currents for better estimation of parameters for dTC inhibition. Each curve was generated from at least three independent oocytes.

Table 2: Apparent K_I Values for dTC Inhibition of ACh- and Suberyldicholine-Evoked Currents in Wild-Type and Mutant Receptors Expressed in *Xenopus* Oocytes[a]

	log IC_{50} ± SEM (M)	IC_{50} (nM)	apparent K_I (nM)
ACh			
WT	−7.07 ± 0.11 (4)	85	41.5
αW86F	−7.06 ± 0.23 (3)	88	4.5
suberyldicholine			
WT	−6.92 ± 0.05 (3)	120	58.3
αW86F	no inhibition		

[a] Log IC_{50} values from individual oocytes were averaged to generate final mean estimates. The value in parentheses is the number of oocytes used for each receptor type.

αW86F mutation was the low amplitude of agonist-evoked currents (see above). We, therefore, investigated whether this was due to a reduced level of receptor expression or a property of a reduced conductance through the mutant receptor channel. Table 3 compares the density of [^{125}I]-α-BgTx binding sites expressed on the oocyte surface to the maximum currents evoked by saturating concentrations of ACh and SbCh. Injection of 50 ng of wild-type subunit cRNAs resulted in a robust expression level of 2−3 fmol of [^{125}I]-α-BgTx binding sites per oocyte. However, receptors carrying the αW86F mutation exhibited a greater than 10-fold decrease in the level of surface expression of [^{125}I]-α-BgTx binding sites. When the maximum currents are normalized to the levels of expression, it appears that the lower currents seen for the mutant receptor can be attributed mainly to reduced levels of expression. Similar experiments were carried out using the αW86A mutant receptor. No

Table 3: Surface Expression and Normalized Maximum Current Seen in Wild-Type and Mutant Receptors Expressed in *Xenopus* Oocytes[a]

	surface binding ± SEM (fmol/oocyte)	I_{max} ± SEM (nA)	normalized peak current (nA/fmol)	% normalized peak current (I_{max}Mut/I_{max}WT)
ACh				
WT	2.9 ± 0.7 (14)	3030 ± 440	1045	100
αW86F	0.2 ± 0.05 (7)	117 ± 32	585.0	56
suberyldicholine				
WT	2.4 ± 0.5 (3)	1310 ± 230	545.8	100
αW86F	0.17 ± 0.01 (3)	100 ± 20	588.2	107

[a] All oocytes were injected with 50 ng of total cRNA. The value in parentheses is the number of oocytes used for each receptor type.

detectable [^{125}I]-α-BgTx binding was measured, thus explaining the lack of detectable current responses with this mutant (see above).

DISCUSSION

The complex effects of bisquaternary compounds acting at the neuromuscular junction and autonomic ganglia have long been recognized (see ref *25*). Early on, it became clear that the distance between the two quaternary ammonium groups of the compound (the interonium distance) was an important factor in determining the pharmacological activity of the ligand (*26*). In the study presented here, we have used site-directed mutagenesis to explore structural features of the *Torpedo* nAChR that may be involved in the recognition of suberyldicholine, a large bisfunctional ligand. Early work on the frog neuromuscular junction revealed SbCh to be an unusually potent agonist (*14*, *15*). Consistent with these results, we report here that SbCh is approximately 8-fold more potent than ACh in activating the wild-type *Torpedo* nAChR expressed in *Xenopus* oocytes (see Table 1). However, in terms of current amplitudes, high concentrations of SbCh evoked only ~50% of the maximum current of ACh; i.e., SbCh acts as a partial agonist. We have previously obtained similar data for agonist-induced flux responses for the *Torpedo* nAChR in native membrane vesicles (S. M. J. Dunn and M. A. Raftery, unpublished observations), suggesting that the partial agonism observed here is not an artifact of the expression system.

As discussed in the introductory section, we previously suggested that differences in the kinetics of binding of SbCh and ACh to the *Torpedo* nAChR may be at least partially attributed to the ability of SbCh to cross-link two subsites existing within each of the two high-affinity binding domains (*16*, *17*). Studies of the association of a series of bisfunctional agonists having different interonium distances led to the suggestion that these subsites may be located ~18 Å apart. Since the ligands that were used were flexible and their bound conformations are unknown, this was an upper estimate based on their extended structures. In the absence of a high-resolution three-dimensional structure of the nAChR, it was impossible to predict the location of this putative secondary subsite for SbCh. More recently, however, the crystal structure of the related protein, the AChBP, has become a valuable template on which to model extracellular structural features of the nAChR (*18*, *27*, 28). The structure of the AChBP (Figure 1B) reveals that a residue that had previously been implicated in ligand recognition by photoaffinity labeling experiments (*8*), i.e., W82 in a position homologous to that of W86 of the *Torpedo* nAChR α subunit, lies approximately 18 Å from other putative binding site residues (Figure 1B). This residue was therefore targeted for mutagenesis in our study of receptor−suberyldicholine interactions.

The tryptophan in the position homologous to αW86 is conserved in all subunits of the LGIC family, suggesting that this residue may have a crucial structural and/or functional role. There is considerable evidence to suggest that it is involved in receptor assembly. Mutations of the homologous Trp121 residue in the homopentameric $5HT_{3A}$ receptor (W121S and W121Y) resulted in a loss of cell surface expression revealed by a lack of both binding and functional responses (*29*). Similarly, in the $GABA_A$ receptor, mutations of this residue in the α1 subunit prevented pentameric assembly of the receptor (*30*). Consistent with these results is the finding that the αW86A mutation led to a complete loss of receptor expression. Functional receptors incorporating the αW86F mutation were, however, expressed on the oocyte surface. Although its expression levels were low, the maximum ACh-evoked current (in terms of nanoamperes per femtomole) of the mutant was not significantly different from that of the wild-type receptor. This suggests that, apart from a reduction in the efficiency of assembly, no global changes in receptor properties had occurred as a consequence of the mutation.

Previously, the role of nAChR αW86 was investigated by substituting unnatural amino acids at this position (*31*). It was concluded that this residue does not contribute to a strong cation−π interaction with ACh since the incorporation of W86 analogues with different electron-withdrawing groups had a <2-fold effect on the EC_{50} value for ACh-induced activation. In agreement with this earlier report, our results show that the αW86F mutation has an only modest effect on ACh-induced activation.

The most significant finding of this study is the dramatic increase in the EC_{50} for SbCh-induced currents (>500-fold) resulting from the αW86F mutation. Furthermore, unlike the responses to ACh, currents evoked by SbCh failed to desensitize and were not blocked by the classical competitive antagonist D-tubocurarine. Thus, αW86 appears to play a crucial role in both SbCh-induced activation and desensitization. Our initial hypothesis was that αW86 may contribute to the formation of a subsite for stabilizing the second quaternary ammonium group of bisquaternary ligands such as SbCh. The simple prediction was, therefore, that mutation of this residue might have a substantial effect on SbCh activation and a weaker effect on activation by ACh and other small monoquaternary agonists. While the results presented above show that this was indeed the case, the lack of either desensitization or dTC inhibition of the SbCh-induced currents is less easily explained. Since the ability

of dTC to inhibit ACh-evoked currents in the mutant receptor was apparently unaltered compared to that of the wild-type receptor, it appears that the mutation does not have a deleterious effect on dTC binding. Assuming that dTC is still able to bind to the well-characterized sites at the $\alpha-\gamma$ and $\alpha-\delta$ subunit interfaces, its lack of ability to inhibit SbCh-evoked responses in the αW86F mutant receptor requires that, in this case, the binding sites for dTC inhibition and SbCh activation are physically distinct. One possibility is that by modifying the secondary binding subsite for SbCh, this ligand can no longer have a high-affinity interaction with the "classical" binding site. Further analysis of this possibility requires a direct determination of whether high-affinity binding sites for SbCh still exist in the mutant receptors. Unfortunately, thus far, the low levels of receptor expression in the oocytes have prevented characterization of the binding of radiolabeled ligands or reliable estimates from the inhibition of [^{125}I]-α-BgTx binding.

If, as a result of the W86F mutation, SbCh can now activate the receptor via a binding site(s) that is distinct from those that bind dTC, the question of the location of this site-(s) arises. In previous studies of the native *Torpedo* nAChR, we made use of covalently bound fluorescent probes to monitor agonist binding. One probe, IANBD (4-{[(iodoacetoxy)ethyl]methylamino}-7-nitro-2,1,3-benzoxadiazole) (*32*−*34*), appears to monitor binding to low-affinity sites that we have correlated with channel activation (*35*, *36*). Curiously, unlike all other agonists that have been examined, the binding of SbCh to fluorescently labeled nAChR was biphasic, suggesting the presence of two classes of binding sites with dissociation constants of ∼2 μM and ∼2 mM (*35*). The higher-affinity one of the two sites seemed to be correlated with receptor activation, but we were unable to assign a role to the very low affinity site(s). While it is attractive to correlate the latter sites with the activating sites in the mutant receptor discussed here, this remains speculative. Previous results of rapid flux experiments using *Torpedo* membranes have also implicated a low-affinity ($EC_{50} \sim 500$ μM) regulatory site for SbCh (but not ACh) in inhibiting ion flux responses (*37*). Similarly, a low-affinity site ($K_d \sim 3$ mM) for SbCh-mediated self-inhibition of efflux of $^{86}Rb^+$ from *Torpedo* membrane vesicles has been reported (*38*). Together, these findings suggest that the nAChR may carry a specific low-affinity site(s) for SbCh, although its role(s) in receptor function remains unclear.

In summary, the results presented above demonstrate that W86 of the nAChR α subunit is an important determinant for receptor activation by the bisquaternary agonist SbCh. We suggest that, in the native receptor, this residue contributes to the formation of a secondary site for binding of bisfunctional ligands.

ACKNOWLEDGMENT

We are indebted to Isabelle Paulsen for her help with these studies. We thank Professors Michael Raftery and Ian Martin for valuable discussions.

REFERENCES

1. Corringer, P. J., Le-Novère, N., and Changeux, J.-P. (2000) Nicotinic receptors at the amino acid level, *Annu. Rev. Pharmacol. Toxicol. 40*, 431−458.
2. Raftery, M. A., Hunkapiller, M. W., Strader, C. D., and Hood, L. E. (1980) Acetylcholine receptor: Complex of homologous subunits, *Science 208*, 1454−1456.
3. Dunn, S. M. J. (1993) Structure and function of the nicotinic acetylcholine receptor, *Adv. Struct. Biol. 2*, 225−244.
4. Arias, H. R. (2000) Localization of agonist and competitive antagonist binding sites on nicotinic acetylcholine receptor, *Neurochem. Int. 36*, 595−645.
5. Karlin, A. (2002) Emerging structure of the nicotinic acetylcholine receptors, *Nat. Neurosci. 3*, 102−114.
6. Kao, P. N., Dwork, A. J., Kaldany, R. R., Silver, M. L., Wideman, J., Stein, S., and Karlin, A. (1984) Identification of the α subunit half-cysteine specifically labeled by an affinity reagent for the acetylcholine receptor binding site, *J. Biol. Chem. 259*, 11662−11665.
7. Dennis, M., Giraudat, J., Kotzyba-Hibert, F., Goeldner, M., Hirth, C., Chang, J. Y., Lazure, C., Chretien, M., and Changeux, J.-P. (1988) Amino acids of the *Torpedo marmorata* acetylcholine receptor α subunit labeled by a photoaffinity ligand for the acetylcholine binding site, *Biochemistry 27*, 2346−2357.
8. Galzi, J.-L., Revah, F., Black, D., Goeldner, M., Hirth, C., and Changeux, J.-P. (1990) Identification of a novel amino acid α-tyrosine 93 within the cholinergic ligands-binding sites of the acetylcholine receptor by photoaffinity labeling. Additional evidence for a three-loop model of the cholinergic ligands-binding sites, *J. Biol. Chem. 265*, 10430−10437.
9. Middleton, R. E., and Cohen, J. B. (1991) Mapping of the acetylcholine binding site of the nicotinic acetylcholine receptor: [^{3}H]Nicotine as an agonist photoaffinity label, *Biochemistry 30*, 6987−6997.
10. Blount, P., and Merlie, J. P. (1989) Molecular basis of the two nonequivalent ligand binding sites of the muscle nicotinic acetylcholine receptor, *Neuron 3*, 349−357.
11. Pedersen, S. E., and Cohen, J. B. (1990) D-Tubocurarine binding sites are located at $\alpha-\gamma$ and $\alpha-\delta$ subunit interfaces of the nicotinic acetylcholine receptor, *Proc. Natl. Acad. Sci. U.S.A. 87*, 2785−2789.
12. Brejc, K., Dijk, W. J. V., Klaassen, R. V., Schuurmans, M., Oost, J. V. D., Smit, A. B., and Sixma, T. K. (2001) Crystal structure of an ACh-binding protein reveals the ligand-binding domain of nicotinic receptors, *Nature 411*, 269−276.
13. Smit, A. B., Syed, N. I., Schaap, D., Van Minnen, J., Klumperman, J., Kits, K. S., Lodder, H., Van Der Schors, R. C., Van Elk, R., Sorgedrager, B., Brejc, K., Sixma, T. K., and Geraerts, W. P. (2001) A glia-derived acetylcholine-binding protein that modulates synaptic transmission, *Nature 411*, 261−268.
14. Dreyer, F., Peper, K., and Sterz, R. (1978) Determination of dose−response curves by quantitative ionophoresis at the frog neuromuscular junction, *J. Physiol. 281*, 395−419.
15. Dionne, V. E., Steinbach, J. H., and Stevens, C. F. (1978) An analysis of the dose−response relationship at voltage-clamped frog neuromuscular junctions, *J. Physiol. 281*, 421−444.
16. Dunn, S. M. J., and Raftery, M. A. (1997) Agonist binding to the *Torpedo* acetylcholine receptor. 1. Complexities revealed by dissociation kinetics, *Biochemistry 36*, 3846−3853.
17. Dunn, S. M. J., and Raftery, M. A. (1997) Agonist binding to the *Torpedo* acetylcholine receptor. 2. Complexities revealed by association kinetics, *Biochemistry 36*, 3854−3863.
18. Celie, P. H., Van Rossum-Fikkert, S. E., Van Dijk, W. J., Brejc, K., Smit, A. B., and Sixma, T. K. (2004) Nicotine and carbamylcholine binding to nicotinic acetylcholine receptors as studied in AChBP crystal structures, *Neuron 41*, 907−914.
19. Goldin, A. L., and Sumikawa, K. (1992) Preparation of RNA for injection into *Xenopus* oocytes, *Methods Enzymol. 207*, 279−297.
20. Barnard, E. A., Miledi, R., and Sumikawa, K. (1982) Translation of exogenous messenger RNA coding for nicotinic acetylcholine receptors produces functional receptors in *Xenopus* oocytes, *Proc. R. Soc. London, Ser. B 215*, 241−246.
21. Miledi, R. (1980) Intracellular calcium and the desensitization of acetylcholine receptors, *Proc. R. Soc. London, Ser. B 209*, 447−452.
22. Sullivan, D. A., and Cohen, J. B. (2000) Mapping the agonist binding site of the nicotinic acetylcholine receptor. Orientation requirements for activation by covalent agonist, *J. Biol. Chem. 275*, 12651−12660.
23. Tamamizu, S., Guzman, G. R., Santiago, J., Rojas, L. V., Mcnamee, M. G., and Lasalde-Dominicci, J. A. (2000) Functional effects of periodic tryptophan substitutions in the α M4 trans-

membrane domain of the *Torpedo californica* nicotinic acetylcholine receptor, *Biochemistry 39*, 4666−4673.
24. Cheng, Y., and Prusoff, W. H. (1973) Relationship between the inhibition constant (K_I) and the concentration of inhibitor which causes 50% inhibition (I_{50}) of an enzymatic reaction, *Biochem. Pharmacol. 22*, 3099−3108.
25. Bovet, D. (1957) The relationships between isosterism and competitive phenomena in the field of drug therapy of the autonomic nervous system and that of neuromuscular transmission, Nobel Lecture, December 11, 1957.
26. Michaelson, M. J., and Zeimal, E. V. (1973) *Acetylcholine: An Approach to the Molecular Mechanisms of* Action, Pergamon Press, Oxford, U.K.
27. Le Novère, N., Grutter, T., and Changeux, J.-P. (2002) Models of the extracellular domain of the nicotinic receptors and of agonist- and Ca^{2+}-binding sites, *Proc. Natl. Acad. Sci. U.S.A. 99*, 3210−3215.
28. Schapira, M., Abagyan, R., and Totrov, M. (2002) Structural model of nicotinic acetylcholine receptor isotypes bound to acetylcholine and nicotine, *BMC Struct. Biol. 2*, 1.
29. Spier, A. D., and Lummis, S. C. (2000) The role of tryptophan residues in the 5-hydroxytryptamine(3) receptor ligand binding domain, *J. Biol. Chem. 275*, 5620−5625.
30. Srinivasan, S., Nichols, C. J., Lawless, G. M., Olsen, R. W., and Tobin, A. J. (1999) Two invariant tryptophans on the α1 subunit define domains necessary for GABA(A) receptor assembly, *J. Biol. Chem. 274*, 26633−26638.
31. Zhong, W., Gallivan, J. P., Zhang, Y., Li, L., Lester, H. A., and Dougherty, D. A. (1998) From *ab initio* quantum mechanics to molecular neurobiology: A cation-π binding site in the nicotinic receptor, *Proc. Natl. Acad. Sci. U.S.A. 95*, 12088−12093.
32. Dunn, S. M. J., and Raftery, M. A. (1982) Activation and desensitization of *Torpedo* acetylcholine receptor: Evidence for separate binding sites, *Proc. Natl. Acad. Sci. U.S.A. 79*, 6757−6761.
33. Dunn, S. M. J., and Raftery, M. A. (1982) Multiple binding sites for agonists on *Torpedo californica* acetylcholine receptor, *Biochemistry 21*, 6264−6272.
34. Dunn, S. M. J., Conti-Tronconi, B. M., and Raftery, M. A. (1983) Separate sites of low and high affinity for agonists on *Torpedo californica* acetylcholine receptor, *Biochemistry 22*, 2512−2518.
35. Dunn, S. M. J., and Raftery, M. A. (1993) Cholinergic binding sites on the pentameric acetylcholine receptor of *Torpedo californica*, *Biochemistry 32*, 8608−8615.
36. Dunn, S. M. J., and Raftery, M. A. (2000) Roles of agonist-binding sites in nicotinic acetylcholine receptor function, *Biochem. Biophys. Res. Commun. 279*, 358−362.
37. Pasquale, E. B., Takeyasu, K., Udgaonkar, J. B., Cash, D. J., Severski, M. C., and Hess, G. P. (1983) Acetylcholine receptor: Evidence for a regulatory binding site in investigations of suberyldicholine-induced transmembrane ion flux in *Electrophorus electricus* membrane vesicles, *Biochemistry 22*, 5967−5973.
38. Forman, S. A., Firestone, L. L., and Miller, K. W. (1987) Is agonist self-inhibition at the nicotinic acetylcholine receptor a nonspecific action? *Biochemistry 26*, 2807−2814.

BI0603773